Information Content of a Single Pass of Phase-Delay Data From a Short Baseline Connected Element Interferometer

S. W. Thurman
Navigation Systems Section

This article presents an analytic development of the information array obtained with a single tracking pass of phase-delay measurements made from a short baseline interferometer. Phase-delay observations can be made with great precision from two antennas using a single, common distributed frequency standard, hence the name "connected element." With the information array, closed-form expressions are developed for the error covariance in declination and right ascension. These equations serve as useful tools for analyzing the relative merits of candidate station locations for connected element interferometry (CEI). The navigation performance of a short baseline interferometer located at the Deep Space Network's (DSN's) Goldstone complex is compared with that which is presently achievable using Very Long Baseline Interferometry (VLBI) over intercontinental baselines. The performance of an intracomplex pair of short baselines formed by three stations is also investigated, along with the use of a single baseline in conjunction with conventional two-way Doppler data. The phase-delay measurement accuracy and data rate used in the analysis are based on the expected performance of an experimental connected element system presently under construction at Goldstone. The results indicate that the VLBI system that will be used during the Galileo mission can determine the declination and right ascension of a distant spacecraft to an accuracy of 20–25 nrad, while the CEI "triad" system and the combination CEI-Doppler system are both capable of 30–70 nrad performance.

I. Introduction

At the present time, wideband delta Very Long Baseline Interferometry (ΔVLBI) is the most accurate angular measurement tool of all the radio metric data types used in deep space navigation. The wideband ΔVLBI system designed for the Galileo mission is capable of angular measurement accuracy in the 20–30 nrad range, which corresponds to a position uncertainty of about 3.0–4.5 km per astronomical unit (AU).[1] Connected element interferometry (CEI) is a new radio interferometric technique in which a common frequency standard, distributed through

[1] *Galileo Navigation Plan*, Galileo Project Document 625-566, Rev. A (internal document), Jet Propulsion Laboratory, Pasadena, California, October 1989.

a fiber-optic communications link to two stations 10–100 km apart, is used to make very precise measurements of the time delay of an incoming signal between the two stations [1,2]. The proximity of the stations makes it possible to observe a spacecraft for 9 to 14 hours, as opposed to the typical 0-to-4-hour view period obtainable with an intercontinental baseline.

In order to compare the relative capabilities of CEI and wideband ΔVLBI, a simple model of the differenced one-way range (DOR) observable, which is theoretically equivalent to both CEI phase-delay and wideband ΔVLBI measurements, was developed and used to form the information array for each data type. The two information arrays were then inverted to obtain closed-form expressions for the error covariance of spacecraft declination and right ascension associated with each tracking model. The use of CEI augmented with two-way Doppler is also investigated, using a simple analytic model for the information contained in a Doppler tracking pass in combination with the CEI information equations. These information models provide a common framework for a comparison of the capabilities of these data types, as a function of some of the key parameters that have an impact on navigation performance.

II. Analysis

Both wideband ΔVLBI and CEI measure the differenced one-way range from a spacecraft to two separate stations, which can be expressed simply as

$$\mathrm{DOR} = \underline{B} \cdot \underline{S} \tag{1}$$

where

$\underline{B}$ = baseline vector $= \underline{r}_1 - \underline{r}_2$

$\underline{r}_1$ = position vector of station 1

$\underline{r}_2$ = position vector of station 2

$\underline{S}$ = unit vector in spacecraft direction

The station locations and baseline components are expressed in cylindrical coordinates in an Earth-fixed frame:

$$\underline{B} = (r_B \cos\lambda_B,\ r_B \sin\lambda_B,\ z_B)$$

where

r_B = baseline component perpendicular to Earth's spin axis

z_B = baseline component parallel to Earth's spin axis

λ_B = baseline longitude

The baseline coordinates as a function of the station coordinates are as follows:

$$\begin{aligned} r_B &= \left[r_1^2 + r_2^2 - 2r_1 r_2 \cos(\lambda_1 - \lambda_2)\right]^{1/2} \\ z_B &= z_1 - z_2 \\ \lambda_B &= \mathrm{Atan}\left[(r_1 \sin\lambda_1 - r_2 \sin\lambda_2)/(r_1 \cos\lambda_1 - r_2 \cos\lambda_2)\right] \end{aligned} \tag{2}$$

where

r_1, r_2 = station location components perpendicular to Earth's spin axis

z_1, z_2 = station location components parallel to Earth's spin axis

λ_1, λ_2 = station longitudes

Using Eq. (2), the DOR observable, Eq. (1), and its partial derivatives can be expressed as a function of the baseline components and the spacecraft coordinates:

$$\mathrm{DOR} = r_B \cos\delta \cos H_B + z_B \sin\delta \tag{3}$$

where

δ = spacecraft declination

$H_B = \alpha_B - \alpha$ (baseline hour angle)

α_B = baseline right ascension

α = spacecraft right ascension

$$\begin{aligned} \partial\mathrm{DOR}/\partial\delta &= -r_B \sin\delta \cos H_B + z_B \cos\delta \\ \partial\mathrm{DOR}/\partial\alpha &= r_B \cos\delta \sin H_B \end{aligned} \tag{4}$$

A. Information Array for DOR Observables

Due to the manner of its implementation, wideband ΔVLBI is typically used to form a single measurement during the time period in which the spacecraft is in view at both stations. Since the baseline is only sensitive to angular displacement in one direction, wideband ΔVLBI observations are made in pairs using two baselines that are as near orthogonal as possible. This is the approach employed for Galileo navigation, with a pair of wideband ΔVLBI measurements being made every three days on average

using the Goldstone–Madrid and Goldstone–Canberra DSN baselines.

The development given below establishes an approximate analytic representation of the error covariance for a pair of wideband ΔVLBI measurements, using the DOR observable model. Since ΔVLBI observations are very sensitive to the effects of the troposphere on the received radio signal, it is desirable to make the measurements at the highest elevation possible for both antennas. To account for this in some respect, the baseline hour angle H is assumed to be 90 deg for both DOR measurements. This assumption simplifies the error covariance equations and has no significant effect on the results obtained from them.

The information content for each DOR measurement is formed using the partial derivatives given in Eq. (4); the two are then summed together to form the complete information array for the two observations. The information content of a single DOR measurement is as follows:

$$I_{\mathrm{DOR}} = \begin{bmatrix} \left(\partial \mathrm{DOR}/\partial\delta\right)^2 & \left(\partial \mathrm{DOR}/\partial\delta\right)\left(\partial \mathrm{DOR}/\partial\alpha\right) \\ \left(\partial \mathrm{DOR}/\partial\delta\right)\left(\partial \mathrm{DOR}/\partial\alpha\right) & \left(\partial \mathrm{DOR}/\partial\alpha\right)^2 \end{bmatrix} \left(2/\sigma^2_{\mathrm{DOR}}\right) \tag{5a}$$

Assuming that no a priori information exists, the error covariance matrix associated with the estimates of δ and α obtained from the DOR observation pair is simply the inverse of the information array:

$$\Gamma_{\mathrm{DOR}} = E\left\{\left(\underline{\mathrm{X}} - \underline{\hat{\mathrm{X}}}\right)\left(\underline{\mathrm{X}} - \underline{\hat{\mathrm{X}}}\right)^{\mathrm{T}}\right\}$$

$$= \begin{bmatrix} \sigma^2_\delta & \sigma^2_{\delta\alpha} \\ \sigma^2_{\delta\alpha} & \sigma^2_\delta \end{bmatrix} = \left(I_{\mathrm{DOR}}\right)^{-1} \tag{5b}$$

where

$$\underline{\mathrm{X}}^{\mathrm{T}} = (\delta, \alpha) \text{ (true values)}$$

$$\underline{\hat{\mathrm{X}}}^{\mathrm{T}} = (\hat{\delta}, \hat{\alpha}) \text{ (estimated values)}$$

Substituting Eq. (4) for Eq. (5a) in each measurement, then adding the two and inverting the resulting DOR information array yields the desired expressions for the elements of the error covariance matrix:

$$\sigma^2_\delta = \left\{ \frac{\left(r^2_{B1} + r^2_{B2}\right)}{\left[\left(r^2_{B1} + r^2_{B2}\right)\left(z^2_{B1} + z^2_{B2}\right) - \left(r_{B1}z_{B1} + r_{B2}z_{B2}\right)^2\right]\cos^2\delta} \right\} \left(\sigma^2_{\mathrm{DOR}}/2\right) \tag{6}$$

$$\sigma^2_\alpha = \left\{ \frac{\left(z^2_{B1} + z^2_{B2}\right)}{\left[\left(r^2_{B1} + r^2_{B2}\right)\left(z^2_{B1} + z^2_{B2}\right) - \left(r_{B1}z_{B1} + r_{B2}z_{B2}\right)^2\right]\cos^2\delta} \right\} \left(\sigma^2_{\mathrm{DOR}}/2\right) \tag{7}$$

$$\sigma^2_{\delta\alpha} = \left\{ \frac{-\left(r_{B1}z_{B1} + r_{B2}z_{B2}\right)}{\left[\left(r^2_{B1} + r^2_{B2}\right)\left(z^2_{B1} + z^2_{B2}\right) - \left(r_{B1}z_{B1} + r_{B2}z_{B2}\right)^2\right]\cos^2\delta} \right\} \left(\sigma^2_{\mathrm{DOR}}/2\right) \tag{8}$$

where

r_{B1}, z_{B1} = radial and z-height components for baseline 1

$r_{B2}, = z_{B2}$ = radial and z-height components for baseline 2

σ^2_{DOR} = variance of DOR observations

B. Information Array for CEI Tracking Pass

The CEI phase-delay observable, like the wideband ΔVLBI observable, is a measurement of differenced one-way range, so the information array for a single measurement is given by Eq. (5a). The information array and associated error covariance matrix for a pass containing N measurements, assuming a constant measurement variance of $\sigma^2{}_{\mathrm{CEI}}$, is then

$$I_{\mathrm{CEI}} = \left[\left(N/\sigma^2_{\mathrm{CEI}}\right) \sum_{i=1}^{N} \left(\partial \mathrm{DOR}_i/\partial \underline{X}\right) \left(\partial \mathrm{DOR}_i/\partial \underline{X}\right)^{\mathrm{T}} \right] \tag{9a}$$

$$\Gamma_{\mathrm{CEI}} = \left(I_{\mathrm{CEI}}\right)^{-1} \tag{9b}$$

where, once again

$$\underline{X}^{\mathrm{T}} = (\delta, \alpha)$$

Equation (9b) is analogous to Eq. (5b) for the DOR observation pair, and it also is based on the assumption that no a priori information exists. The summation in Eq. (9a) can be replaced with integration, assuming continuous observations. The resulting integrals can then be adjusted by a constant to account for the fact that the observations are discrete. For example, the information element for declination becomes

$$I_{\mathrm{CEI\ 11}} = \left(1/\omega^2{}_{\mathrm{CEI}}\Delta t\right) \int_{\mathrm{A}}^{\mathrm{B}} \left(\partial \mathrm{DOR}/\partial \delta\right)^2 dH \tag{10}$$

where

ω = Earth rotation rate

Δt = time interval between measurements

The variable Δt forces the integrated information element to be equivalent to the corresponding summed element. Since the variable of integration is the baseline hour angle H_B, careful consideration must be given to the choice of the limits A and B. The baseline hour angle can be defined in terms of the hour angle of one end of the baseline, chosen to be station 2 here, as follows:

$$H_B = H + \phi \tag{11}$$

where

H_B = baseline hour angle

H = station 2 hour angle

ϕ = baseline longitude relative to station 2

$$\phi = \lambda_B - \lambda_2 = \mathrm{Atan}\left[r_1 \sin(\lambda_1 - \lambda_2)/(r_1 \cos(\lambda_1 - \lambda_2) - r_2)\right] \tag{12}$$

Equation (12) was obtained by setting λ_2 to zero in Eq. (2) and replacing λ_1 with $(\lambda_1 - \lambda_2)$. Using Eqs. (11) and (12), the limits of integration for the elements of the information array can be expressed in terms of the hour angle of station 2. If it is further assumed that the two stations comprising the connected element are near enough to each other such that the hour angle for both stations is roughly the same, then the limits can be expressed in terms of a single station hour angle and the baseline angle ϕ:

$$A = -H + \phi$$

$$B = H + \phi \tag{13}$$

where

H = tracking pass half-width

The information array for a single, symmetric (in H) CEI tracking pass is then

$$I_{CEI} = \begin{bmatrix} I_{\mathrm{CEI\ 11}} & I_{\mathrm{CEI\ 12}} \\ I_{\mathrm{CEI\ 12}} & I_{\mathrm{CEI\ 22}} \end{bmatrix}$$

$$I_{\mathrm{CEI\ 11}} = \left(J_1 r_B^2 \sin^2\delta + J_2 z_B^2 \cos^2\delta - 2J_3 r_B z_B \sin\delta \cos\delta\right) / \left(\omega \sigma^2_{\mathrm{CEI}} \Delta t\right) \tag{14}$$

$$I_{\mathrm{CEI\ 12}} = \left(J_4 r_B z_B \cos^2\delta - J_5 r_B^2 \sin\delta \cos\delta\right) / \left(\omega \sigma^2_{\mathrm{CEI}} \Delta t\right)$$

$$I_{\mathrm{CEI\ 22}} = \left(J_6 r_B^2 \cos^2\delta\right) / \left(\omega \sigma^2_{\mathrm{CEI}} \Delta t\right)$$

where

$$J_1 = H + (1/2)\sin 2H \cos 2\phi$$

$$J_2 = 2H$$

$$J_3 = 2\cos\phi \sin H \tag{15}$$

$$J_4 = 2\sin\phi \sin H$$

$$J_5 = \sin 2\phi \sin 2H$$

$$J_6 = H - (1/2)\sin 2H \cos 2\phi$$

It must be noted that Eqs. (14) and (15) were developed assuming that the declination δ and the right ascension α of the spacecraft are constant during the tracking period. While this is a reasonable assumption for a single pass, which takes place during the course of several hours, it is not applicable when it is desired to accumulate a sequence of CEI tracking passes taking place over a period of several days. To do so requires a more sophisticated model for the spacecraft state variables which includes the rates of change of α and δ.

The error covariance of the spacecraft angular coordinates can now be obtained by inverting the CEI information array, Eq. (14):

$$\sigma_\delta^2 = \frac{H - (1/2)\sin 2H \cos 2\phi}{D_1 r_B^2 \sin^2\delta + D_2 z_B^2 \cos^2\delta + D_3 r_B z_B \sin\delta\cos\delta} \left(\omega\sigma_{\text{CEI}}^2 \Delta t\right) \tag{16}$$

$$\sigma_\alpha^2 = \frac{[H + (1/2)\sin 2H\cos 2\phi] r_B^2 \sin^2\delta + 2H z_B^2 \cos^2\delta - 4\cos\phi \sin H r_B z_B \sin\delta\cos\delta}{D_1 r_B^4 \sin^2\delta\cos^2\delta + D_2 r_B^2 z_B^2 \cos^4\delta + D_3 r_B^3 z_B \sin\delta\cos^3\delta} \left(\omega\sigma_{\text{CEI}}^2 \Delta t\right) \tag{17}$$

$$\sigma_{\delta\alpha}^2 = \frac{2\sin\phi \sin H z_B \cos\delta - \sin 2\phi \sin 2H r_B \sin\delta}{D_1 r_B^3 \sin^2\delta\cos\delta + D_2 r_B z_B^2 \cos^3\delta + D_3 r_B^2 z_B \sin\delta\cos^2\delta} \left(\omega\sigma_{\text{CEI}}^2 \Delta t\right) \tag{18}$$

where

$$D_1 = H^2 - \sin^2 2H \left[\sin^2 2\phi + (1/4)\cos^2 2\phi\right]$$

$$D_2 = 2H\left[H - (1/2)\sin 2H \cos 2\phi\right] - 4\sin^2\phi \sin^2 H$$

$$D_3 = \sin H \sin 2H \left(2\sin\phi \sin 2\phi + \cos\phi\cos 2\phi\right)$$

$$- 2H\cos\phi \sin H \tag{19}$$

C. Information Array for Doppler Tracking Pass

The Doppler information model given below was developed by Hamilton and Melbourne in their classic 1966 paper [3]. Over the course of a single tracking period, the range-rate to a distant spacecraft observed at a station can be closely approximated by the following expression:

$$\dot\rho = \dot r + \omega r_s \cos\delta \sin H \tag{20}$$

where

$\dot\rho$ = station–spacecraft range-rate

$\dot r$ = spacecraft geocentric range-rate

r_s = station component perpendicular to Earth's spin axis

In Eq. (20), H and δ are the spacecraft hour angle and declination, respectively, just as in the DOR and CEI tracking models. The Doppler signal is seen to be a function of the three spacecraft coordinates $\dot r$, δ, and α. The information array for a single, symmetric pass ($-H$ to $+H$) of data is

$$\mathrm{I}_{\text{DOP}} = \left[(N/\sigma_{\dot\rho}^2)\sum_{i=1}^{N} (\partial\dot\rho_i/\partial\underline{\mathrm{X}})\,(\partial\dot\rho_i/\partial\underline{\mathrm{X}})^{\mathrm{T}}\right] = \mathbf{A}^{\mathrm{T}}\mathbf{J}\mathbf{A} \tag{21}$$

where

$$\underline{\mathrm{X}}^{\mathrm{T}} = (\dot r, \delta, \alpha)$$

$$\mathbf{A} = \begin{bmatrix} 1 & 0 & 0 \\ 0 & -\omega r_s \sin\delta & 0 \\ 0 & 0 & -\omega r_s \cos\delta \end{bmatrix} \tag{22}$$

$$\mathbf{J} = \begin{bmatrix} 2H & 0 & 2\sin H \\ 0 & H - (1/2)\sin 2H & 0 \\ 2\sin H & 0 & H + (1/2)\sin 2H \end{bmatrix} \times \left(\frac{1}{\omega \sigma_\rho^2 \Delta t} \right) \tag{23}$$

Inversion of Eq. (21) yields expressions for the variance of the declination and right ascension estimates obtained from the tracking pass. In the equations given below, the effects of timing and station location errors on the estimates are included.

$$\sigma_\delta^2 = (1/\sin^2 \delta) \left\{ \frac{(\sigma_\rho^2 \Delta t / \omega r_s^2)}{[H - (1/2)\sin 2H]} + \cos^2 \delta \, (\sigma_{r_s}^2 / r_s^2) \right\} \tag{24}$$

$$\sigma_\alpha^2 = (\sigma_\rho^2 \Delta t / \omega r_s^2 \cos^2 \delta) \times \left\{ H / \left[H^2 + (1/2) H \sin 2H - 2\sin^2 H \right] \right\} + \omega^2 \sigma_\tau^2 + \sigma_\delta^2 \tag{25}$$

$$\sigma_{\delta\alpha}^2 = 0 \tag{26}$$

where

σ_ρ^2 = range-rate measurement variance

Δt = time interval between data points

σ_τ^2 = variance of timing error

σ_λ^2 = variance of station longitude error

D. Tracking Pass Width as a Function of Declination

Before comparing CEI and VLBI navigation performance, the selection of an appropriate value for the tracking pass half-width, H, must be addressed. Edwards [2] has shown that random fluctuations in the troposphere are probably the dominant error source in determining CEI phase-delay measurement accuracy, and that the statistical uncertainty of this effect is inversely proportional to the elevation angle at which the spacecraft is being observed. His analysis indicates that the troposphere-induced measurement uncertainty drops off exponentially with increasing elevation, with most occurring within the elevation angle at which the spacecraft is being observed. His analysis indicates that the troposphere-induced measurement uncertainty drops off exponentially with increasing elevation, with most occurring within the elevation range 0–30 deg. To account for this variation, the tracking pass half-width H can be made to vary with declination such that the spacecraft is only observed when its elevation angle is above some minimum. An elevation cutoff of 30 deg was chosen for use here, based on the above discussion. At this elevation, the phase-delay uncertainty due to tropospheric fluctuations is about 5 mm. Admittedly this is a somewhat arbitrary selection; nevertheless, the use of this value should yield some reasonable indication of how the navigation performance obtained from CEI varies with declination.

To some degree this same argument also applies to Doppler data since they are also affected adversely by random tropospheric fluctuations. An elevation cutoff of 15 deg has been commonly used during past flight projects—and was used below for all scenarios involving Doppler. Since Doppler data can be readily acquired by all of the stations within the Deep Space Network (DSN), which are located in both the northern and southern hemispheres, the declination of the spacecraft being tracked is of little importance in terms of its effect on tracking pass width.

Elevation can be expressed directly as a function of declination, hour angle, and station location as

$$h = \mathbf{A} \sin \left[(r_s/\zeta) / \cos\delta \cos H + (z/\zeta) \sin \delta \right] \tag{27}$$

where

h = elevation angle

r_s = station location spin radius, as in Eq. (2)

z = station location z-height, Eq. (2)

$\zeta = (r_s^2 + z^2)^{1/2}$

Figure 1 shows the variation in tracking pass half-width with declination for minimum elevations of 10–30 deg. As seen in Fig. 1, the reduction in pass width becomes especially pronounced as declination drops below zero. These curves, or curves corresponding to other stations when appropriate, were used to determine the value of H to use in all of the results involving CEI and Doppler data which follow.

III. Results

A reference VLBI tracking scenario was created using the DOR error covariance equations, Eqs. (6) through (8),

to obtain the uncertainty for a pair of observations taken from the baselines formed by DSN Goldstone–Madrid (DSS 14–63) stations and Goldstone-Canberra (DSS 14–43) stations. These two baselines are the most nearly orthogonal set possible within the Deep Space Network. The measurement accuracy assumed for both DOR observations was 14 cm (1σ), which is the performance expected for the wideband ΔVLBI system carried by the Galileo spacecraft.[2] The baseline coordinates and results for this case are given in Table 1. In this scenario it was assumed that $\delta = 0$, making this a best-case result.

Actual wideband ΔVLBI measurements are constructed by differencing a spacecraft DOR observation with a second DOR observation of an extragalactic radio source (EGRS), which is normally a quasar. This results in the cancellation, or near-cancellation, of the effects of certain error sources that are common to both stations. The locations of quasars used for ΔVLBI are usually very well known, but not exactly known, and so this uncertainty must be considered in determining the overall accuracy of ΔVLBI measurements. Current quasar catalogs are known to be accurate to 5–15 nrad [4]. To account for this uncertainty in some sense, the results in Table 1 consist of the root-sum-square uncertainty of the right ascension (RA) and declination (DEC) uncertainties obtained from the ΔVLBI measurements plus a 15-nrad quasar location uncertainty.

A CEI tracking scenario, also for $\delta = 0$, was constructed for comparison, using a fictitious north–south baseline ($\phi = 0$) 20.5 km in length, with one end being DSS 15 at Goldstone. The baseline coordinates and results for this scenario are given in Table 2. A scale map of the Goldstone Deep Space Communications Complex (DSCC) appears in Fig. 2, showing DSS 15 at the north end.[3] Admittedly, the construction of a 20.5-km north–south baseline would require a station located outside of the present boundaries of the Goldstone DSCC, shown in the lower left-hand corner of Fig. 2. This fictitious station would not be far outside the current boundary, though, and since the construction of any operational CEI system would probably depend upon the construction of new stations in any event, this assumed station location is reasonable for the purposes of this analysis.

Actual CEI measurements will consist of a spacecraft phase-delay measurement differenced with a quasar phase-delay measurement, similar to ΔVLBI observations, and for essentially the same reasons—to obtain cancellation of common error sources. As with the VLBI results in Table 1, the CEI accuracy figures in Table 2 also contain a 15-nrad quasar location uncertainty in both RA and DEC, combined in a root-sum-square sense with the uncertainties obtained from the measurements themselves. It should be noted here that quasar location uncertainty was not a significant contributor to navigation error uncertainty in any of the VLBI or CEI cases considered herein.

Table 2 illustrates an important point: a single north–south CEI baseline can determine both declination and right ascension. Figures 3 and 4 show the effects of rotating the baseline away from a north–south orientation as a function of spacecraft declination. By the conventions chosen in defining ϕ, Eq. (12), a negative value of ϕ implies a rotation of the baseline to the west from north, while a positive value of ϕ implies a rotation to the east from north. Only curves for positive values of ϕ are shown, since a negative ϕ yields a covariance of the same magnitude as the corresponding ϕ of opposite sign. From these two figures, it can be seen that rotating the baseline away from a north–south orientation causes some degradation in both σ_δ and σ_α, but it is not significant except for low (less than $-10°$) declination and for baseline angles greater than roughly $\pm 20°$. Figure 4 shows that the capability of a north–south baseline to determine RA decreases rapidly with decreasing declination. Finger and Edwards,[4] in their numerical investigation of CEI tracking performance from Goldstone baselines, obtained similar results, but their analysis was restricted to declinations of $-23°$, $0°$, and $+23°$.

If a third station were added to the single baseline two-station CEI system envisioned thus far, two separate baselines could be formed into a connected element "triad." Figure 5 is a diagram showing such a hypothetical system at Goldstone, with the third station situated just outside the southeast corner of the complex. This system incorporates an east–west baseline with the original north–south baseline. Table 3 contains the baseline coordinates of the system and the tracking results which would be obtained for a spacecraft at 0° declination. In these scenarios, the error covariance for the combined tracking solution from the two baselines is computed by adding the information arrays obtained for each individual baseline, then inverting the result. The combined information from the two baselines reduces the RA uncertainty obtained with just the north–south baseline from 107 nrad to about 42 nrad,

[2] Ibid.

[3] Based on *Directory of Goldstone Buildings and Facilities*, JPL Project Document 890-165, Rev. A (internal document), Jet Propulsion Laboratory, Pasadena, California, October 1, 1989.

[4] M. H. Finger and C. D. Edwards, "Relative CEI Navigation Performance of Goldstone Intracomplex Baselines," Interoffice Memorandum 335.3-88-116 (internal document), Jet Propulsion Laboratory, Pasadena, California, October 20, 1988.

a factor of 2.5 improvement. This suggests that a CEI triad system could determine both RA and DEC to better than 50 nrad, using data taken only by stations at a single complex—in this case, Goldstone.

When used in conjunction with other data types, a single north–south CEI baseline may yet be a valuable navigation tool. The use of X-band (8.4 GHz) frequencies for both the uplink and downlink communications legs with the Magellan spacecraft, and later for Galileo and Mars Observer, should yield Doppler measurements of range-rate accurate to 0.1 mm/sec or better, except in cases where the Sun-Earth-probe angle is less than 15°.[5] Current Doppler accuracy for S-band (2.3 GHz) spacecraft communications is in the 0.5–1.0 mm/sec range. Table 4 describes the navigation accuracy which would be obtained with a combination of X-band Doppler passes from stations at the DSN sites in Madrid, Spain, and Canberra, Australia, with CEI data from Goldstone, again for a spacecraft at 0° declination. The values used in Table 4 for timing error (σ_τ) and station spin radius (σ_{r_s}) and longitude errors (σ_λ) are somewhat optimistic by current standards, but they should be attained within the next few years. As in the CEI triad scenario, the error covariance for the combined CEI-Doppler solution is simply the inverse of the summed information obtained from each data type. The addition of the Doppler data in this case results in a factor of 2 improvement in RA uncertainty over the performance of the north–south CEI baseline alone, from 107 nrad to 53 nrad.

Figure 6 is a comparison of the error uncertainty ellipses for the tracking scenarios given in Tables 1–4. The orientations of the VLBI ellipse reflects the orientations of the baselines that comprise the system, while it is apparent that the CEI systems and the CEI–Doppler combination both produce uncorrelated error covariances for δ and α. Table 5 provides a comparison of the navigation performance obtained from each of the three tracking systems discussed here, ΔVLBI, CEI triad and CEI-Doppler, as declination varies from −20° to +20°. Figures 7 and 8 present the information in Table 5 graphically. In these tables and figures, "CEI+Dop" refers to the tracking system described in Table 4, which uses data from a single north–south Goldstone CEI baseline in combination with Doppler data from Madrid and Canberra. Remember that in all of these cases, the tracking pass half-width is also changing with declination, so the variations seen in Table 4 are actually a function of two parameters, H and δ, not just δ.

[5] P. W. Kinman and J. G. Meeker, "Two-Way Coherent Doppler Measurement Accuracy for Venus Radar Mapper," Interoffice Memorandum 3392-84-94 (internal document), Jet Propulsion Laboratory, Pasadena, California, July 6, 1984.

IV. Conclusions

This study used simple, approximate mathematical models to investigate the relative tracking performance obtainable with two interferometric methods—a hypothetical CEI triad system at Goldstone and the wideband ΔVLBI system which will be used by the Galileo spacecraft—and a third hybrid system that uses a single CEI baseline in conjunction with conventional Doppler. The analysis performed indicates that the Galileo ΔVLBI system is capable of determining both RA and DEC to 20–25 nrad throughout the ecliptic plane. The hypothetical Goldstone intracomplex CEI system, which comprises three stations, is capable of producing sub-50–nrad estimates of DEC throughout the ecliptic plane, and RA estimates of 50 nrad accuracy or better down to a declination of about −10°. Data from even a single Goldstone connected element interferometer, when combined with X-band Doppler data from two other DSN stations, are capable of determining DEC to better than 50-nrad throughout the ecliptic plane and RA to 50–70 nrad.

The results of this study show that intracomplex CEI is a viable alternative to ΔVLBI for missions requiring spacecraft angular coordinate determination to an accuracy of 30–50 nrad. While the navigation accuracy achievable with intracomplex CEI from the Goldstone DSCC suffers somewhat at very low declinations, it has been shown that even a single 20.5-km baseline at Goldstone can potentially deliver better than 70-nrad accuracy when used in conjunction with X-band (8.4 GHz) Doppler. If a CEI system were also built at the DSN Canberra complex, this low declination problem would be eliminated. Considering the speed and reliability with which phase-delay data can be generated and processed for navigation, CEI can provide the DSN with a tremendous capability, in terms of both the number of missions that can be supported simultaneously and the navigation accuracy that can be achieved.

References

[1] C. D. Edwards, "Angular Navigation on Short Baselines Using Phase Delay Interferometry," *IEEE Transactions on Instrumentation and Measurement*, vol. 38, no. 2, pp. 665–667, April 1989.

[2] C. D. Edwards, "The Effect of Spatial and Temporal Wet-Troposphere Fluctuations on Connected Element Interferometry," *TDA Progress Report 42-97*, vol. January–March 1989, Jet Propulsion Laboratory, Pasadena, California, pp. 47–57, March 15, 1989.

[3] T. W. Hamilton and W. G. Melbourne, "Information Content of a Single Pass of Doppler Data from a Distant Spacecraft, *JPL Space Programs Summary*, vol. 3, no. 37–39, Jet Propulsion Laboratory, Pasadena, California, pp. 18–23, March–April 1966.

[4] O. J. Sovers, C. D. Edwards, C. S. Jacobs, G. E. Lanyi, K. M. Liewer, and R. N. Treuhaft, "Astrometric Results of 1978–1985 Deep Space Network Radio Interferometry: The JPL 1987-1 Extragalactic Source Catalog," *The Astronomical Journal*, vol. 95, no. 6, pp. 1647–1658, June 1988.

Table 1. VLBI tracking scenario results ($\delta = 0$)

Baseline	r_B, km	z_B, km
Goldstone–Madrid	8378.986	−341.545
Goldstone–Canberra	7620.841	7351.800

Measurement accuracy σ_{DOR} = 14 cm (approx. 20 nrad)

Quasar direction uncertainty (1σ) = 15 nrad (in both declination and right ascension)

σ_δ = 24.2 nrad
σ_α = 19.4 nrad

Table 2. CEI tracking scenario results ($\delta = 0$)

Baseline: r_B = 11.467 km, z_B = 17.000 km, $\phi = 0$, length = 20.61 km
(Station 1 is DSS 15, Goldstone, California)

Tracking pass half-width $H = 52.3°$
(elevation cutoff = 30°)

Time interval between measurements Δt = 360 sec

Earth rotation rate $\omega = 7.292 \times 10^{-5}$ rad/sec

Measurement accuracy σ_{CEI} = 5 mm (approx. 250 nrad)

Quasar direction uncertainty (1σ) = 15 nrad

σ_δ = 38.4 nrad
σ_α = 107 nrad

Table 3. CEI triad system performance ($\delta = 0$)

Baseline	r_B, km	z_B, km	ϕ, deg	Length, km
1: North–south	11.647	17.000	0.0	20.61
2: East–west	12.000	0.0	90.0	12.00

For all baselines:
$H = 52.3°$ (elevation cutoff = 30°), Δt = 360 sec, σ_{CEI} = 5 mm

$\omega = 7.292 \times 10^{-5}$ rad/sec
Quasar direction uncertainty (1σ) = 15 nrad

σ_δ = 31.6 nrad
σ_α = 42.4 nrad

Table 4. Combined X-band Doppler–CEI performance ($\delta = 0$)

Doppler data: Station	r_B, km	z, km	λ, deg	H, deg
DSS 42, Canberra	5205.352	−3674.582	148.9813	71.5
DSS 62, Madrid	4860.817	4116.906	355.6322	70.2

CEI baseline:
r_B = 11.467 km, z_B = 17.000 km, $\phi = 0°$
$H = 52.3°$ (elevation cutoff = 30°), Δt = 360 sec, σ_{CEI} = 5 mm

Δt = 60 sec, $\sigma_{\dot\rho}$ = 0.1 mm/sec, elevation cutoff = 15°
$\omega\sigma_\tau$ = 20 nrad, σ_λ = 60 nrad, σ_{r_s} = 30 cm

σ_δ = 35.3 nrad
σ_α = 52.9 nrad

Table 5. Relative performance comparison between systems

δ(°)	DEC uncertainty, nrad			RA uncertainty, nrad		
	VLBI	CEI triad	CEI+Dop	VLBI	CEI triad	CEI+Dop
−20	25.2	40.7	46.6	19.9	68.3	67.5
−15	24.8	35.2	39.7	19.7	55.1	62.7
−10	24.4	32.9	37.4	19.5	48.7	58.5
−5	24.3	31.9	36.1	19.5	44.9	55.3
0	24.2	31.6	35.3	19.4	42.4	52.9
5	24.3	31.7	34.8	19.5	40.9	51.2
10	24.4	32.3	34.7	19.5	40.0	50.0
15	24.8	33.2	34.6	19.7	39.6	49.3
20	25.2	34.5	34.7	19.9	39.6	48.9

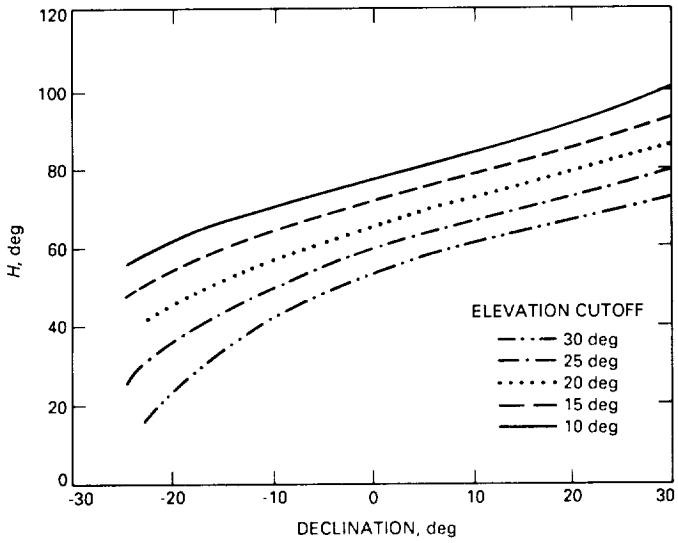

Fig. 1. Tracking pass half-width versus spacecraft declination for different elevation cutoffs (DSS 15, Goldstone, California).

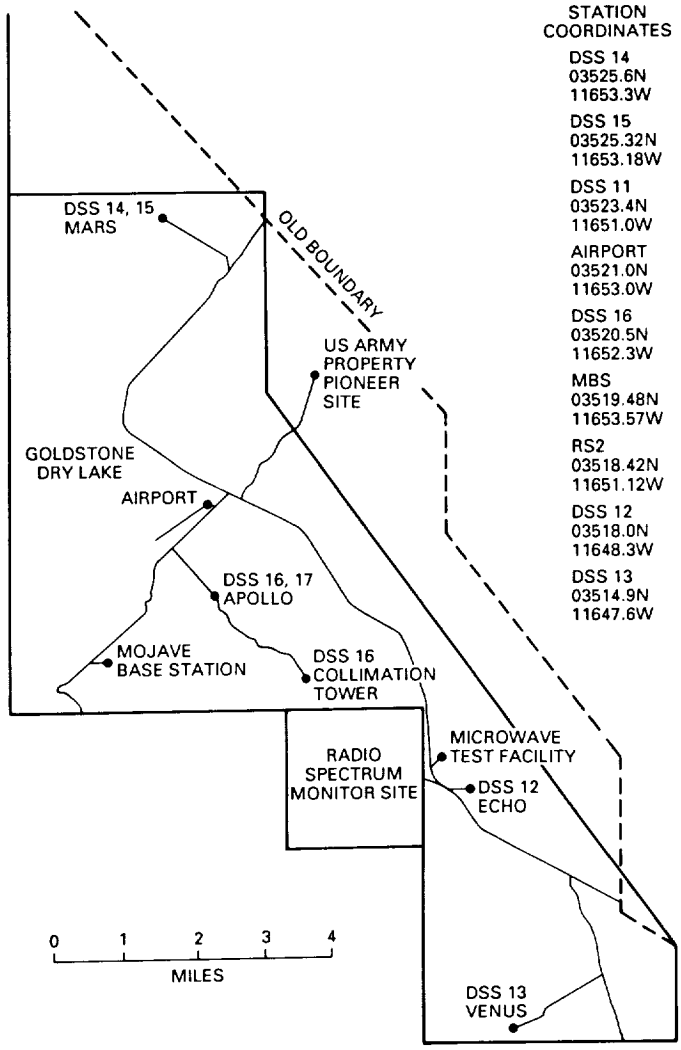

Fig. 2. Goldstone Deep Space Communications Complex.

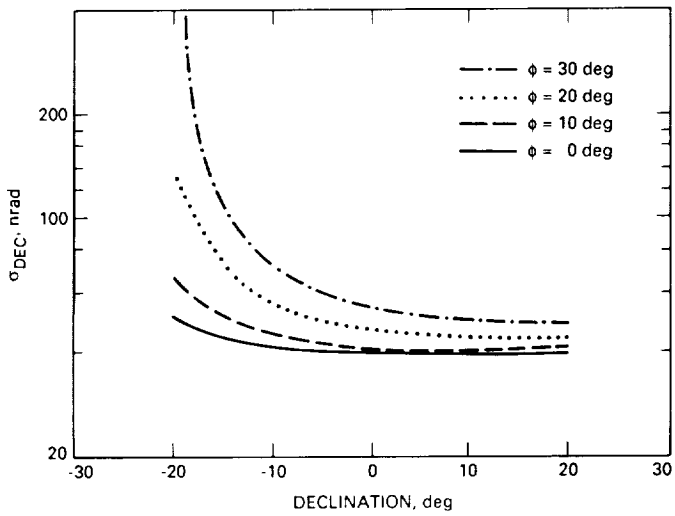

Fig. 3. DEC uncertainty versus declination for a north-south Goldstone CEI baseline.

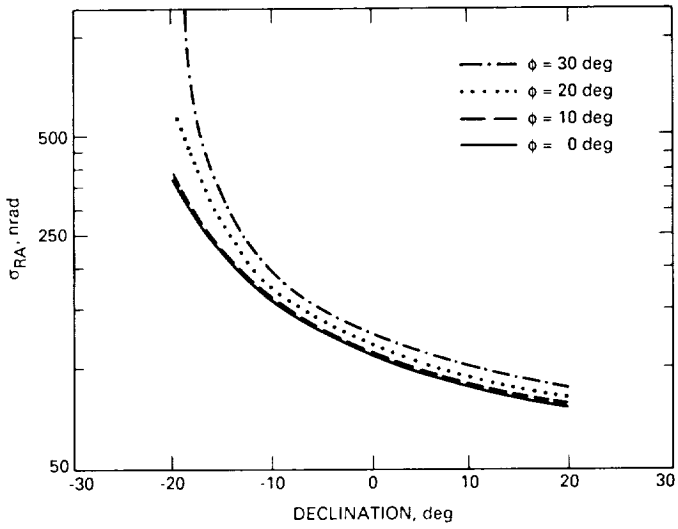

Fig. 4. RA uncertainty versus declination for a north-south Goldstone CEI baseline.

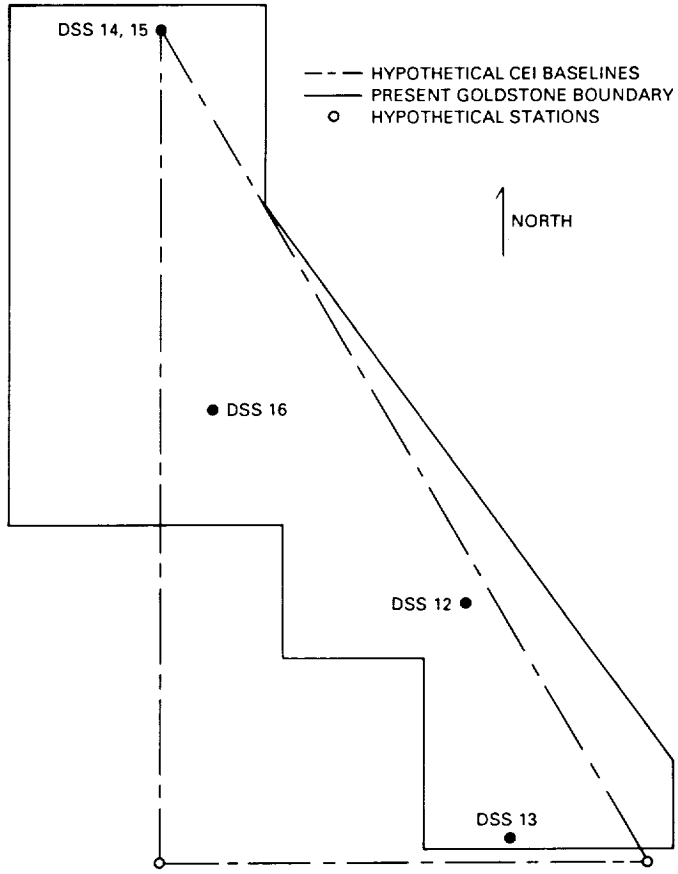

Fig. 5. Layout of hypothetical Goldstone CEI triad system.

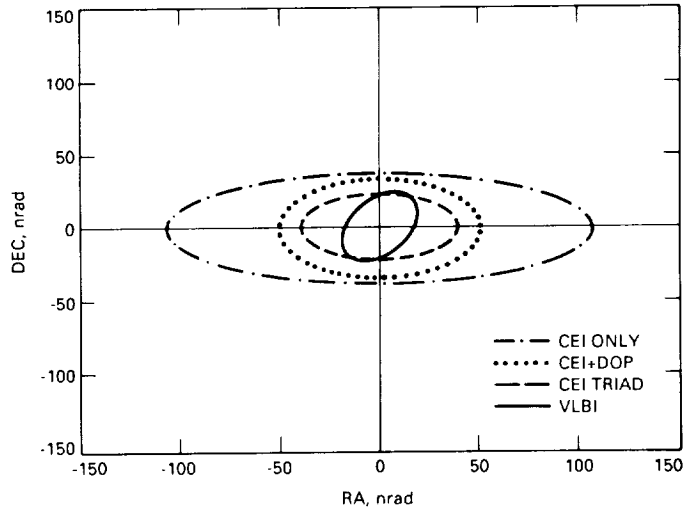

Fig. 6. Uncertainty ellipses for CEI and VLBI tracking scenarios ($\delta = 0°$).

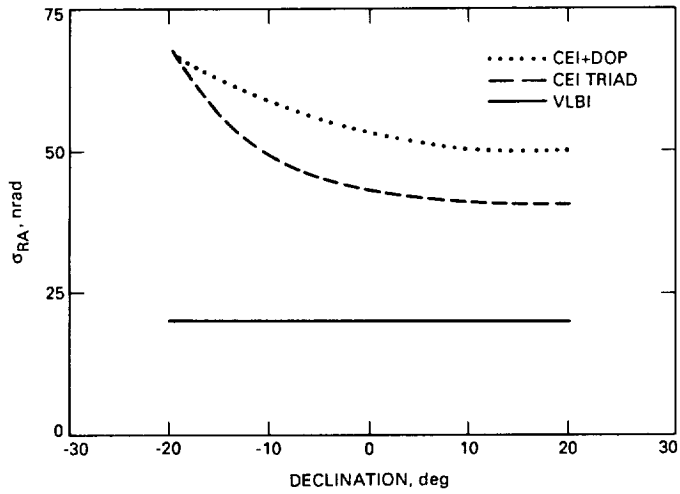

Fig. 7. RA uncertainty versus declination for VLBI, CEI triad, and CEI+Doppler systems.

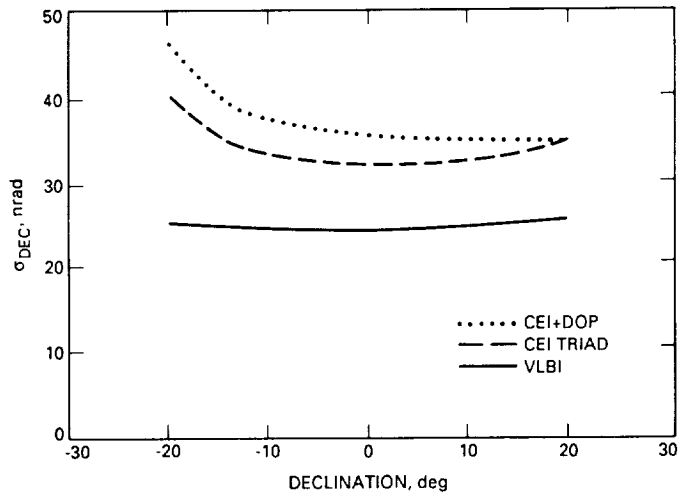

Fig. 8. DEC uncertainty versus declination for VLBI, CEI triad, and CEI+Doppler systems.